

A practical method to avoid bond crossing in two-dimensional dissipative particle dynamics simulations

Cite as: J. Chem. Phys. **129**, 024902 (2008); <https://doi.org/10.1063/1.2953694>

Submitted: 25 April 2008 . Accepted: 10 June 2008 . Published Online: 10 July 2008

Hong Liu, Yao-Hong Xue, Hu-Jun Qian, Zhong-Yuan Lu, and Chia-Chung Sun



View Online



Export Citation

ARTICLES YOU MAY BE INTERESTED IN

Dissipative particle dynamics: Bridging the gap between atomistic and mesoscopic simulation

The Journal of Chemical Physics **107**, 4423 (1997); <https://doi.org/10.1063/1.474784>

Perspective: Dissipative particle dynamics

The Journal of Chemical Physics **146**, 150901 (2017); <https://doi.org/10.1063/1.4979514>

Dynamics of entangled linear polymer melts: A molecular-dynamics simulation

The Journal of Chemical Physics **92**, 5057 (1990); <https://doi.org/10.1063/1.458541>

Lock-in Amplifiers up to 600 MHz

starting at

\$6,210



Zurich
Instruments

Watch the Video



A practical method to avoid bond crossing in two-dimensional dissipative particle dynamics simulations

Hong Liu,¹ Yao-Hong Xue,² Hu-Jun Qian,¹ Zhong-Yuan Lu,^{1,a)} and Chia-Chung Sun¹

¹State Key Laboratory of Theoretical and Computational Chemistry, Institute of Theoretical Chemistry, Jilin University, Changchun 130023, China

²Institute of Mathematics, Jilin University, Changchun 130012, China

(Received 25 April 2008; accepted 10 June 2008; published online 10 July 2008)

Dissipative particle dynamics (DPD) simulation technique is an effective method targeted on mesoscopic simulations in which the interactions between particles are soft. As a result, it inevitably causes bond crossing and interpenetration between particles. Here we develop a practical method based on the two-dimensional DPD model which can extremely reduce the possibility of bond crossing. A rigid core is added to each particle by modifying the form of the conservative force in DPD so that the particles cannot penetrate each other. Then by adjusting the spring constant of the bond, we can impose a simple geometry constraint so that the bond crossing can hardly take place. Furthermore, we take into account an analytic geometry constraint in the polymerization model of DPD by which we can successfully avoid the severe bond crossing problem during bond generation in two dimensions. A parabola fitting between the pressure and the particle number density shows that our modified DPD model with small rigid cores can still be mapped onto the Flory–Huggins model, and the mesoscopic length scale of our simulations does not change. By analyzing the mean-square displacement of the innermost monomer and the center of mass of the chains, we find a $t^{8/15}$ power law of the polymer dynamics in our model instead of the Rouse prediction supporting the recent results in literature. © 2008 American Institute of Physics. [DOI: 10.1063/1.2953694]

I. INTRODUCTION

In recent years, the behavior of two-dimensional (2D) polymers have attracted more and more attention. In many areas, the 2D system has its significant relations such as the strongly adsorbed polymers, ultrathin polymer layers in lubricated contacts between the solids, and so on.¹ According to Semenov and Johner,¹ there are two distinct models describing polymers in two dimensions, i.e., the strictly self-avoiding polymer chains [self-avoiding walks (SAWs)] and the partially self-avoiding chains [self-avoiding trails^{2,3} (SATs)]. The chain intersections are forbidden in the SAW model but allowed in the SAT model. The SAW model corresponds to polymer monolayers such as strongly adsorbed chain systems, whereas the SAT model is used to describe the ultrathin polymer multilayers. SAWs can be considered as the extreme condition of SATs.

In this paper, we mainly consider the SAW model in which the chains cannot overlap with each other so that there should be no bond crossing between the chains. It is actually a technical difficulty to avoid the bond crossing of 2D models with soft interaction potentials. As an effective simulation technique, dissipative particle dynamics (DPD) had been successfully applied in mesoscopic simulations for several years.^{4–15} In this method, all particles interact with each other via three pairwise forces (the conservative, the dissipative, and the random forces) so that the momentum of the system is conserved. As a result, the DPD method can repro-

duce the correct hydrodynamic behavior of fluids. This handling ensures that the system reaches the thermodynamic equilibrium state much easier and that the kinetic trapping is partially eliminated. However, the soft interparticle potential also results in the possibility of bond crossing among the chains and further leads to the incorrect polymer dynamical behavior. This is a critical issue in three dimensions and even more severe in 2D simulations.

There were some successful attempts that had been developed to solve the bond crossing problem in recent years. For example, Briels^{16,17} and co-workers considered the entangled bonds as elastic bands and then determined the entanglement positions by calculating the energy minimization. Pan and Manke¹⁸ introduced the segmental repulsive forces between the points of nearest contact of the chains to reduce the frequency of bond crossing. Recently, Nikunen *et al.*¹⁹ presented a smart method to avoid bond crossing simply by increasing the value of the DPD interaction parameter α_{ij} and the spring constant C accordingly.

In this paper, we develop a practical method to extremely reduce the possibility of bond crossing and avoid the particle interpenetration problem based on the standard DPD model. In this method, we add a rigid core to each DPD particle so that the particles cannot penetrate each other. Then we use a simple geometrical constraint to avoid bond crossing among polymer chains in two dimensions similar to that used by Nikunen *et al.*¹⁹ Moreover, generating well-distributed chain configurations without bond crossing is a hard task. Here, we suggest an analytic geometry condition together with the idea of polymerization to avoid the possi-

^{a)}Author to whom correspondence should be addressed. Electronic mail: luzhy@mail.jlu.edu.cn.

bility that the newly generated bond crosses with the preexisting bonds. The algorithm is proved to be feasible and efficient. Actually, this approach can be used in any simulation models when they are used to study the 2D polymerizations. The paper is organized as follows: Sec. II exhibits the computational details of our model, Sec. III shows the simulation results by using this modified DPD model and the corresponding discussion, and finally, Sec. IV presents the concluding remarks.

II. SIMULATION METHOD AND MODEL CONSTRUCTION

A. The standard DPD method

In the standard DPD method, the time evolution of the interacting particles is governed by Newton's equation of motion.⁴ Interparticle interactions are characterized by pairwise conservative, dissipative, and random forces acting on a particle i by a particle j . They are given by

$$\begin{aligned}\mathbf{F}_{ij}^C &= -\alpha_{ij}\omega^C(r_{ij})\mathbf{e}_{ij}, \\ \mathbf{F}_{ij}^D &= -\gamma\omega^D(r_{ij})(\mathbf{v}_{ij} \cdot \mathbf{e}_{ij})\mathbf{e}_{ij}, \\ \mathbf{F}_{ij}^R &= \sigma\omega^R(r_{ij})\xi_{ij}\Delta t^{-1/2}\mathbf{e}_{ij},\end{aligned}\quad (1)$$

where $\mathbf{r}_{ij} = \mathbf{r}_i - \mathbf{r}_j$, $r_{ij} = |\mathbf{r}_{ij}|$, $\mathbf{e}_{ij} = \mathbf{r}_{ij}/r_{ij}$, and $\mathbf{v}_{ij} = \mathbf{v}_i - \mathbf{v}_j$. ξ_{ij} is a random number with zero mean and unit variance. α_{ij} is the repulsion strength, which always takes the value of 25 for the particles of the same kind in the simulations.⁴ $\omega^C(r_{ij}) = 1 - r_{ij}$ for $r_{ij} < 1$ and $\omega^C(r_{ij}) = 0$ for $r_{ij} \geq 1$ such that the conservative forces are soft and repulsive. The weight functions $\omega^D(r_{ij})$ and $\omega^R(r_{ij})$ of the dissipative and random forces couple together to form a thermostat. Español and Warren²⁰ showed the correct relations between the two functions

$$\begin{aligned}\omega^D(r) &= [\omega^R(r)]^2, \\ \sigma^2 &= 2\gamma k_B T.\end{aligned}\quad (2)$$

We take a simple choice of $\omega^D(r)$ due to Groot and Warren,⁴

$$\omega^D(r) = [\omega^R(r)]^2 = \begin{cases} (1-r)^2 & (r < 1) \\ 0 & (r \geq 1) \end{cases}. \quad (3)$$

It should be noted that the choice of $\omega(r_{ij})$ is not unique and is the simplest form adopted here because of its common usage in roughly all published works.

GW-VV algorithm^{4,5} is used for numerical integration

$$\begin{aligned}\mathbf{r}_i(t + \Delta t) &= \mathbf{r}_i(t) + \Delta t \mathbf{v}_i(t) + 1/2(\Delta t)^2 \mathbf{f}_i(t), \\ \tilde{\mathbf{v}}_i(t + \Delta t) &= \mathbf{v}_i(t) + \lambda \Delta t \mathbf{f}_i(t), \\ \mathbf{f}_i(t + \Delta t) &= \mathbf{f}_i[\mathbf{r}(t + \Delta t), \tilde{\mathbf{v}}(t + \Delta t)], \\ \mathbf{v}_i(t + \Delta t) &= \mathbf{v}_i(t) + 1/2\Delta t[\mathbf{f}_i(t) + \mathbf{f}_i(t + \Delta t)].\end{aligned}\quad (4)$$

Here $\lambda = 0.65$ according to Ref. 5.

In our simulations, the radius of interaction, the particle mass, and the temperature are set to be unity, i.e., $r_c = m = kT = 1$. Polymers are constructed by connecting the neigh-

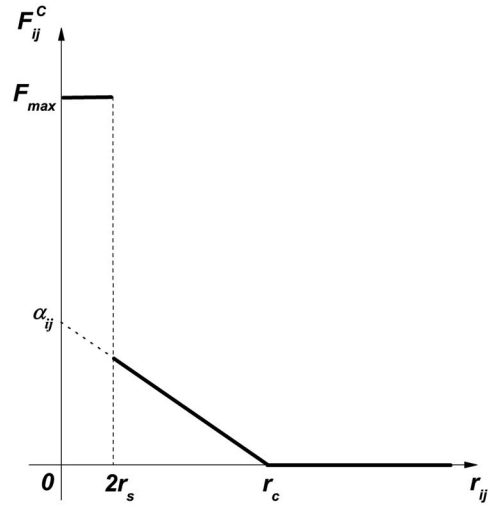


FIG. 1. Sketch of the piecewise conservative force F_{ij}^C between the particles in the modified DPD model.

boring particles together via the harmonic springs with $\mathbf{F}_i^S = \sum_j C(\mathbf{r}_{ij} - \mathbf{r}_e)$, where $r_e = |\mathbf{r}_e|$ is the equilibrium bond length. A 2D box of size 100×100 with periodic boundary conditions is adopted in the simulations. The particle number density ρ is set to 2.

B. Controlling the bond crossing in DPD

As a kind of appropriate mesoscopic simulation method, DPD is efficient and promising. However, because of the soft nature of its interaction potential, it inevitably causes bond crossing and interpenetration between particles, which is unphysical in the real polymer systems. Pan and Manke¹⁸ suggested a segmental repulsion model for DPD so that the segmental repulsive force forms a cylinder of repulsion around each segment of the polymer chain to avoid the interchain cross. Here we adopt a similar handling. In our method, we add a rigid core to each DPD particle by modifying the conservative force so that the particles cannot penetrate each other. Now the conservative force is

$$\mathbf{F}_{ij}^C = \begin{cases} F_{\max} \mathbf{e}_{ij} & (r_{ij} < 2r_s) \\ \alpha_{ij}(1 - r_{ij}/r_c) \mathbf{e}_{ij} & (2r_s \leq r_{ij} \leq r_c), \\ 0 & (r_{ij} > r_c) \end{cases}, \quad (5)$$

where r_s is the preset value of the rigid core radius added to the particles. F_{\max} is a preset constant, which brings a large but finite potential barrier to the overlapping particles. When the distance between a pair of particles r_{ij} is less than the preset rigid core diameter $2r_s$, it will suffer a large force F_{\max} . It should be noted that the value of F_{\max} should be set neither too large nor too small. If F_{\max} is too small, the pair of touched particles i and j (it means that the two cores of the particle pair touch each other and the distance r_{ij} is just the diameter $2r_s$) may move closer to a great extent because the repulsive interaction is not strong enough. On the contrary, if F_{\max} is too large, there will be a large impulse on the momentum of the system, which cannot be omitted. In this study, we choose the value of F_{\max} about two to four times larger than α_{ij} . Figure 1 describes the modified conservative

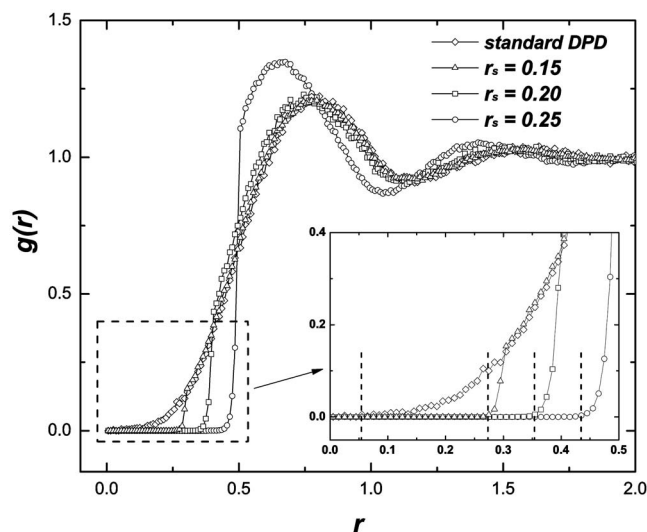


FIG. 2. RDF of the monomer systems when we add the rigid cores to the particles. The RDF of the monomer system in standard DPD is also shown for comparison.

force between two DPD particles. With this modification, the time step Δt in the simulation should be decreased accordingly, and we find $\Delta t = 0.002$ as a proper value.

Since the value of F_{\max} is finite, the rigid cores of the particles may be penetrated more or less. As a result, the actual rigid core radius r_0 should be a little smaller than the preset value r_s . Therefore, we use the radial distribution function (RDF) to check the actual value of r_0 practically. We choose the position that corresponds to the first nonzero value in RDF as $2r_0$ because the distance of the particles cannot be smaller than $2r_0$ in any case. Figure 2 shows the RDFs of monomers with different sizes of rigid cores in our model. The RDF of monomers calculated by using the standard DPD is also shown in Fig. 2 for comparison. It is clear that in standard DPD (i.e., without the rigid core), the smallest distance between the particles is even close to zero (the diamonds in Fig. 2). However, when we add the rigid core to the particles, their smallest distance increases with the increase in r_s , and the value of $2r_0$ is near the corresponding preset diameter $2r_s$. As shown in Fig. 2, the first peak positions of the RDFs with $r_s = 0.20, 0.15$, and 0 (i.e., the standard DPD) approximately coincide with each other at $r = 0.78$, whereas the first peak position of the RDF with $r_s = 0.25$ is obviously smaller ($r = 0.67$). It can be attributed that the particles with larger rigid cores tend to be stuck to their local positions. In a limited case, the particles with rigid core radius equal to $1/(2 + \sqrt{2}) \approx 0.293$ will be arranged in a 2D crystal-like structure at $\rho = 2$. Thus, the first peak of its RDF should appear at around 0.6 indicating the coordinating position of the innermost shell of the particles for this 2D crystal-like structure. In our simulations, the preset radius $r_s = 0.25$ is a relatively large value and close to the limiting value of 0.293 . It corresponds to a large rigid core size so that the movements of the particles are partially frozen as in the case of the rigid core radius being equal to 0.293 . Consequently, we find that the first RDF peak appears at around 0.67 . Actually, the rigid core r_0 should not be chosen too large via adopting a large r_s ; otherwise, the simulation cannot

be mapped onto the Flory–Huggins theory anymore.⁴ Consequently, the length scale of the simulation may change. This issue will be discussed in detail in the next section.

It should be noted that in the simulations, we choose the particle number density of the system $\rho = 2$ so that the particles in the simulation box are not too crowded to move. Ortiz *et al.*²¹ indicated in their DPD study that the densities of different types of particles are not identical when mapping the DPD sites to the coarse-grained polymers and that some unphysical results may appear in the DPD simulation with typical high densities. Similarly, Nikunen *et al.*¹⁹ chose a much lower density $\rho = 1$ in their simulations. Thus, we believe that it is rational to choose $\rho = 2$ in our 2D simulations.

Now we try to avoid the bond crossing in two dimensions following the work of Nikunen *et al.*¹⁹ In Ref. 19, the authors considered a simple geometry constraint condition, i.e., if the condition $\sqrt{2}r_{\min} > l_{\max}$ is satisfied in three dimensions, two bonds cannot cross each other. Here r_{\min} equals the rigid core diameter $2r_0$ and l_{\max} is the maximum stretch of bonds. Similarly, by increasing the spring constant C , we get larger spring forces among the chain particles so that l_{\max} is limited to a proper value. It should be noted that the equilibrium bond length r_e should be changed to $2r_0$ instead of $r_e = 0$ in the standard DPD.⁴ Practically, we obtain l_{\max} by constructing the bond length distribution in a series of simulations. The maximum value in the distribution corresponds to the maximum stretch of the bond l_{\max} . For each set of parameters, we simulate a polymer system with 2×10^4 particles for 5×10^5 time steps. Subsequently, the bond length distribution is obtained by the standard time average. Thus, the geometry constraint conditions are $\sqrt{2} \cdot 2r_0 > l_{\max}$ in three dimensions and $4r_0 > l_{\max}$ in two dimensions. In three dimensions, the particles are confined to the condition of volume exclusion of their spatial configurations, as shown in Fig. 3(a). However, in two dimensions, the particles are confined to the condition of planar exclusion, as shown in Fig. 3(b). If $l_{\max} < 4r_0$ can be satisfied in two dimensions, the distance between two connected particles is less than $2r_0$ according to Fig. 3(b), and any other particle cannot go through the space in between these two particles.

In our 2D simulations, we have adjusted the spring constant C to a large value so that the bond length is short enough to satisfy $4r_0 > l_{\max}$. It should be noted that in the work of Nikunen *et al.*,¹⁹ they defined an operational 0.05 criterion, i.e., the mean-square deviation of the bond length l_s must be smaller than 0.05 to guarantee the correct behavior. In their simulations, the average bond length is always larger than the preset equilibrium bond length $l = 0.95$. Moreover, they found that l_s and l_{\max} both decrease with increasing repulsion strength α_{ij} . On the contrary, r_{\min} increases with increasing α_{ij} . Therefore, it is possible to define a criterion of l_s that guarantees $l_{\max} < \sqrt{2}r_{\min}$. However, we find in our simulations that l_s , l_{\max} , and r_{\min} all increase with increasing F_{\max} . Therefore, it is impossible for us to define a similar 0.05 criterion as used in Ref. 19. This discussion can also be applied to the operational definition of the rigid core radius r_0 obtained from RDFs. In our simulations, we have not observed the apparent dependence of r_0 on the simulation time. So we directly choose the position that corresponds to the

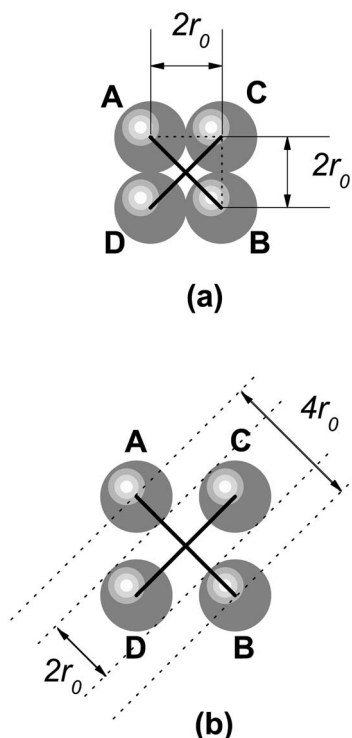


FIG. 3. The schematic representation of the geometry constraint condition of the bond crossing in (a) three dimensions and (b) two dimensions.

first nonzero value of RDF as $2r_0$. The following two sets of parameters are chosen for comparison: (1) $F_{\max}=100$, $r_s=0.15$, and $C=300$; and (2) $F_{\max}=100$, $r_s=0.25$, and $C=500$. We find that in set (2) the condition of $4r_0 > l_{\max}$ can be strictly satisfied, so there is no bond crossing in this set. However, there are some difficulties in set (1) to satisfy the constraint condition. Specifically, there are approximately 0.05% of the bond lengths that are slightly longer than the value of $4r_0$ although we have adjusted the spring constant C to a relatively large value. Nevertheless, we have not observed any bond crossing in the 2D systems simulated for 10^7 time steps. Therefore, we can only conclude that the possibility of bond crossing in set (1) is effectively decreased. Although the critical condition of the constraint cannot be perfectly satisfied, we find that bond crossing does not take place in 1×10^6 time steps of simulation. If a bond crossing takes place—for example, particle **A** crosses from one side of the bond **CD** to the other side to form the crossed bonds in Fig. 3(b)—**A** has to be in the middle of the space between particles **C** and **D** and moves through the space along the direction perpendicular to the bond **CD**. We think it is nearly impossible since there is a strong repulsive potential between the particles **C** and **D**. Moreover, it is obvious that in two dimensions, the crossing of two inner chain bonds requires at least five particles to crowd in a very small region. However, it is basically impossible with such a hard interaction. Comparatively, the chain end is easier to cross with other chains than the inner monomer of the chain since the movement of the end is restricted by only one monomer connecting to it. However, the number of chain ends is a small value in the polymer systems, and the end moving along the direction perpendicular to the bond is very scarce.

All of these factors determine that there is practically no bond crossing in our simulations with parameter set (1) even though the constraint condition $4r_0 > l_{\max}$ cannot be strictly satisfied. However, parameter set (1) is evaluated better than parameter set (2) since the model with set (2) cannot be mapped onto the Flory–Huggins theory, as shown in Sec. III B. Thus, in the following simulations, parameter set (1) will always be chosen as otherwise indicated.

C. Avoiding bond crossing during 2D chain configuration generation

In Sec. II C, we have presented the modifications of the DPD model to avoid unphysical bond crossing in the polymer melts. However, there is still another critical issue when we try to generate the reasonable initial chain configurations in two dimensions, especially for long chains. In the simulations, we always hope that the initial chain configurations are as representative as possible so that the system is easier to equilibrate. However, in two dimensions, we cannot generate the chain configurations simply by randomly putting the polymer chains in a rectangular box since bond crossing will definitely take place. Worse, when a newly generated bond crosses with a preexisting one in two dimensions, the cross will always exist and the behaviors of these two chains are totally correlated. Actually, it is a severe problem for any 2D simulations with long polymer chains. Certainly, one way to avoid this problem is to put the chains regularly in the simulation box as they are in crystals. However, the systems with regular chain configurations in our test simulations cost an extremely long computational time to relax. Thus, this method is not acceptable, especially for long polymer chains.

We suggest an analytic geometry method together with the idea of polymerization²² to solve this problem. The polymerization begins with the original configuration of randomly distributed free monomers, a few being considered as the initiated free radicals and the others as common monomers. In the simulations, if an active end (the free radicals are considered original active ends) meets several free monomers in the reaction radius, it randomly chooses one of the monomers as a reacting object, and they are connected together to finish the step of local polymerization. Subsequently, the active end is transferred to the latter monomer to continue the process of chain propagation. We adopt this idea to generate our chain configurations in two dimensions. The key issue is to control the process so that newly generated bonds do not cross all the preexisting bonds in each chain propagation step.

First, it is necessary to find the condition that two line segments cross each other in the analytic geometry model. As shown in Fig. 3(b), the parameter equations of the two crossing line segments are

$$\begin{aligned} \mathbf{f}_1(t) &= t\mathbf{A} + (1-t)\mathbf{B} \quad (0 \leq t \leq 1), \\ \mathbf{f}_2(t) &= t\mathbf{C} + (1-t)\mathbf{D} \quad (0 \leq t \leq 1). \end{aligned} \quad (6)$$

A, **B**, **C**, and **D** are the terminal points of the two line

segments. Suppose the position coordinates are $\mathbf{A}=(x_A, y_A)$, $\mathbf{B}=(x_B, y_B)$, $\mathbf{C}=(x_C, y_C)$, and $\mathbf{D}=(x_D, y_D)$. If they have a meeting point, there should be a specific $t_1(0 \leq t_1 \leq 1)$ and $t_2(0 \leq t_2 \leq 1)$ so that $\mathbf{f}_1(t_1)=\mathbf{f}_2(t_2)$ can be satisfied. Then we get

$$(\mathbf{A} - \mathbf{B})t_1 + (\mathbf{D} - \mathbf{C})t_2 = \mathbf{D} - \mathbf{B}. \quad (7)$$

Suppose

$$\begin{aligned} \mathbf{A} - \mathbf{B} &= (x_A - x_B, y_A - y_B) = (m, n), \\ \mathbf{D} - \mathbf{C} &= (x_D - x_C, y_D - y_C) = (p, q), \end{aligned} \quad (8)$$

$$\mathbf{D} - \mathbf{B} = (x_D - x_B, y_D - y_B) = (u, v),$$

then Eq. (7) turns out to be

$$\begin{cases} mt_1 + pt_2 = u \\ nt_1 + qt_2 = v. \end{cases} \quad (9)$$

Therefore, $t_1 = (uq - pv)/(mq - np)$ and $t_2 = (mv - nu)/(mq - np)$. If the obtained t_1 and t_2 are in the interval $[0, 1]$, the two line segments will surely cross each other.

During the polymerization process in our simulations, when the active end finds a free monomer in the reaction radius (taken the same as r_c), we assume that the bond can be generated. Then we take the active end as the center and search for any preexisting bonds around it. All of the detected bonds are taken as line segments and combined with the newly generated bond to form a pair. We then calculate the values of t_1 and t_2 for all these pairs. If there is a pair of t_1 and t_2 that can satisfy the condition $t_1 \in [0, 1]$ and $t_2 \in [0, 1]$ simultaneously, we can judge that the newly generated bond must cross the chosen existing bond. Then we discard this trial bond generation and continue until the active end finds a monomer with which the bond does not cross. The process of chain generation is composed of thousands of such steps with bond crossing discrimination. The algorithm is proved to be feasible and efficient, and we have obtained the chain configurations, which present a good starting point for further 2D simulations. It should be noted that this approach is not restricted to our modified DPD model but can be used in any simulation models when they are aimed to study the 2D polymer systems with long chain lengths.

III. SIMULATION RESULTS AND DISCUSSION

A. A primary inspection of the configuration

In this study, we have applied the modified DPD model to simulate strictly 2D polymer chain melts. Figure 4 shows a typical configuration for chain length $N=100$ after 10^6 simulation steps as an exhibition. For eligible observation, we only present a local scene in the simulation box with size 30×30 . We can see that the bond crossing is successfully eliminated by applying our modified DPD model. All the chains are kept separated from each other. In the previous reports, there are some arguments on the 2D chain configuration without bond crossing. Meyer *et al.*²³ implied in their

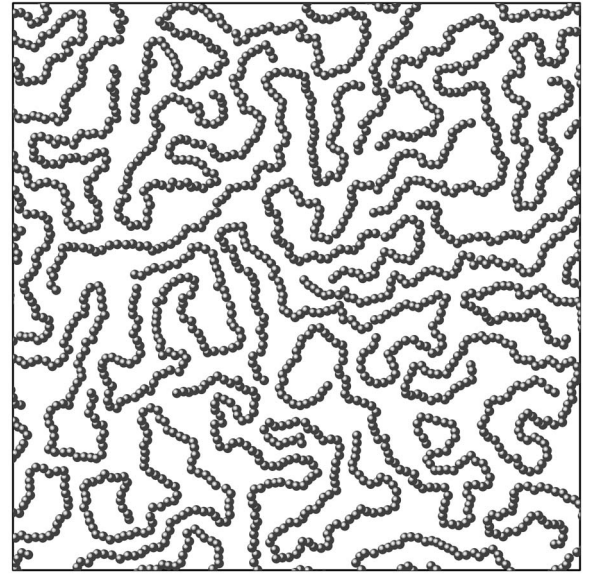


FIG. 4. Snapshot of a typical configuration for a chain with $N=100$. For clarity, we only show a fraction of size 30×30 out of the simulation box.

paper that the individually separated chains are disklike objects. Semenov and Johner¹ also indicated that each chain fills a close region and adopts a segregated pancake conformation, and the chains may keep the behavior as an ameboid motion. However, the results of Cavallo *et al.*²⁴ disapproved this viewpoint, which indicated that the chains typically do not adopt segregated disklike shapes and are much more elongated and irregular. In our simulations, the configuration of the chains seems neither elongated nor enclosed. Some of the chains may stretch their parts to the region of others, adopting the expanding wirelike conformation. However, some chains may retrace to form a semiclosed shape while differing from the so-called disklike conformation. We believe that this mixed state with the diversity of chain configurations profits to the entropy increase of the system and thus reduces the free energy.

B. Mapping onto Flory–Huggins

Groot and Warren⁴ presented a successful parabola fitting between the pressure and the particle number density in their standard DPD method

$$p = \rho k_B T + \kappa \rho^2 \quad (\rho > 2), \quad (10)$$

where κ is the fitting parameter. Consequently, they mapped the DPD model onto the Flory–Huggins theory and made a link between the DPD repulsion parameters and Flory–Huggins χ parameters. Such mapping implies that DPD method is suitable to study the mesoscopic coarse-grained polymer systems. We have also measured the dependence of the system pressure on the particle number density to check if our modified DPD method can still be mapped onto the Flory–Huggins theory. We calculate the pressure according to the virial theorem as²⁵

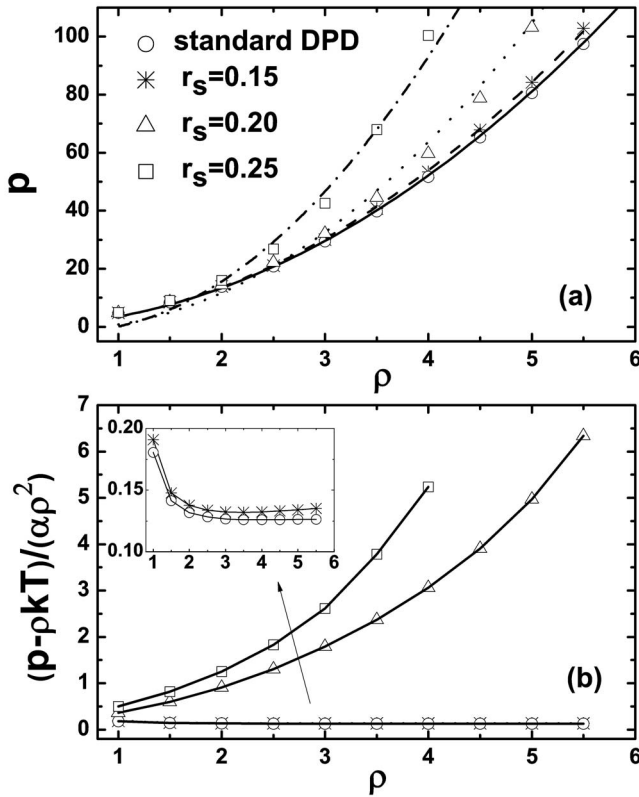


FIG. 5. (a) Pressures obtained from the simulations of standard and modified DPD models (symbols) and the corresponding parabola fits (lines). (b) P divided by $\alpha \rho^2$, which is calculated from (a). All results are obtained with the parameter $\alpha_{ij} = 25$.

$$P = \frac{1}{2} \sum_{\nu} P_{\nu\nu},$$

$$P_{\nu\nu} = \frac{1}{V} \left(\sum_i p_{i\nu} p_{i\nu} / m_i + \sum_i \sum_{j>i} r_{ij\nu} f_{ij\nu} \right), \quad (11)$$

$$p_{i\nu} = m_i v_{i\nu},$$

where $\nu = X, Y$ in two dimensions. Figure 5 shows the relation between the calculated average pressure and the number density of the standard and modified DPD models. It should be noted that if the density of the system is too large, the particles with rigid cores will become too crowded in the simulation box and suffer from very strong repulsions; thus, we collect the data below the density value $\rho \leq 5.5$ (for even larger rigid radius, for example $r_s = 0.25$, we collect the data below $\rho \leq 4$) (see Fig. 5). All of the results are obtained with the preset parameter $F_{\max} = 100$. From Fig. 5, we can find that the preset radius r_s is a very sensitive parameter in our modified DPD model and strongly influences the relation between P and ρ . It is obvious that the data from the standard and modified DPD models with $r_s = 0.15$ can both fit well the parabola function in Eq. (10), whereas the data from the modified DPD model with $r_s = 0.20$ and $r_s = 0.25$ cannot be fitted in Eq. (10). It should be noted that the parabola fitting curves for the data from the standard and modified DPD models with $r_s = 0.15$ are slightly different from each other. Nevertheless, in these two cases, the relationship between the

pressure and the number density can be described well by the Flory–Huggins-type equation of state, which implies that the intrinsic length scale of the modified DPD model with $r_s = 0.15$ is on mesoscale, the same as that of the standard DPD model. However, as shown in Fig. 5(b), we cannot find the plateau regions for the modified DPD model with $r_s = 0.20$ and $r_s = 0.25$. It indicates that the value of the preset rigid radius r_s is a sensitive parameter for defining the length scale of the model. We find that $r_s = 0.15$ is a proper value for the modified DPD model by which the mesoscopic length scale of the model is kept and the possibility for bond crossing is extremely reduced.

The results on the sensitive influence of r_s on the length scale of the simulation model imply that it is difficult to span the different length scales within a single simulation method. Therefore, the multiscale simulations combining various simulation techniques in different length scales are urgently needed for a better understanding of the relation between the microscopic molecular structures and the macroscopic properties. The standard DPD model facilitates the study of mesoscopic structures of soft matter since it can be mapped well onto the Flory–Huggins model. As a consequence of the phenomenological coarse graining, the dynamic properties of the soft matter are not easily and correctly investigated in the standard DPD model. By tuning up the bead rigidity to avoid bond crossing, we find that the modified DPD model suggested here can be mapped onto the Flory–Huggins theory and extremely reduce the possibility of bond crossing with $r_s = 0.15$. However, if we try to satisfy strictly the relation $4r_0 > l_{\max}$ by increasing r_s , the pressure cannot be fitted by a parabola function of ρ . Higher term dependence of P on ρ is actually similar to a virial expansion for a classical fluid, which means that the microscopic interaction characteristics should be considered.²⁶ Thus, to focus on the dynamics of a polymer chain, we have to decrease the level of coarse graining by taking into account the molecular details. By doing this, however, the mesoscopic simulation technique will turn to be microscopic. Similarly, we find that the model of Nikunen *et al.*¹⁹ is also low level coarse grained and its length scale tends to be microscopic with a low particle number density $\rho = 1$, which is similar to our model with larger preset radius r_s .

C. Study of the diffusion dynamics

Semenov and Johner¹ indicated in their study that in strictly two dimensions, the polymer chain relaxation is controlled mainly by the friction at the coil boundary rather than each monomer being a source of friction. This prediction implies that the application of the Rouse model in 2D melts is not necessarily true. A particular power law that the chain relaxation time t_N scales with N as $t_N \sim t_1 N^{15/8}$ instead of the square dependence that $t_N \sim t_1 N^2$ of the Rouse time²⁷ was suggested. Later, Meyer *et al.*²³ tested this prediction in their simulations by analyzing the mean-square displacement (MSD) of the innermost monomer of a chain $g_i(t)$. They indicated that for displacements inside the volume pervaded by a chain, the distance covered by a monomer in time t should be proportional to $R_g(N)$, so they expected to find the

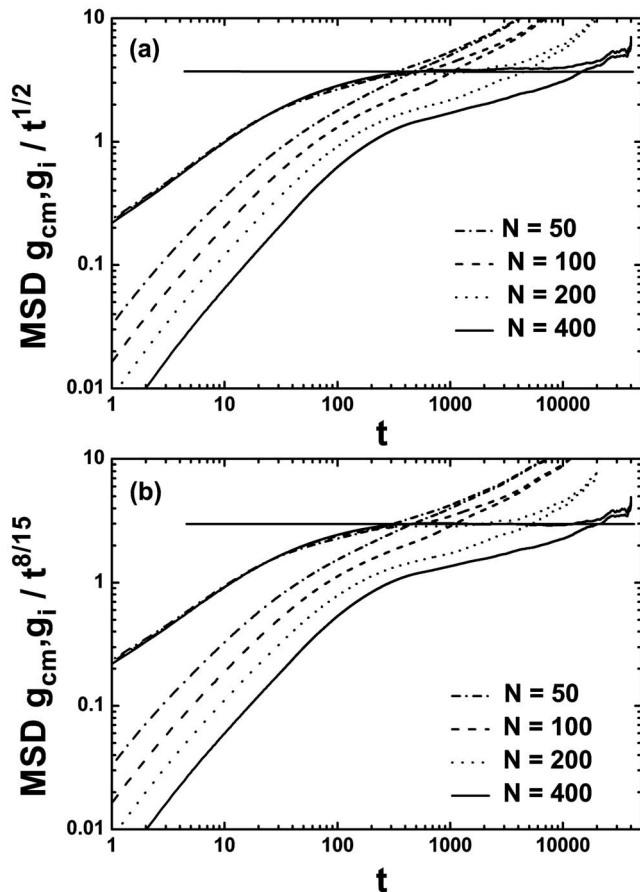


FIG. 6. Time evolution of the MSDs of the center of mass $g_{cm}(t)$ and of the innermost monomer $g_i(t)$ divided by (a) $t^{1/2}$ and (b) $t^{8/15}$, respectively.

power law $g_i(t) \sim R_g^2(N) \sim N \sim t^{8/15}$ instead of the Rouse prediction $g_i(t) \sim t^{1/2}$. In their study, they found that the prediction agrees well with their simulation. We quote this method to test if our 2D model can also prove this prediction. Figure 6 shows the MSDs of the center of mass $g_{cm}(t)$ and of the innermost monomer $g_i(t)$ during the 10^4 DPD time units of the simulations. The MSDs are divided by $t^{1/2}$ and $t^{8/15}$ in Figs. 6(a) and 6(b), respectively. In both figures, it is obvious that in early stages, the MSDs of the innermost monomers $g_i(t)$ for all N values can fit together very well, which implies that the subdiffusive behaviors of the innermost monomers in chains of different lengths can obey the same diffusion dynamics and are immune from the influence of that actual chain length. At later times, $g_i(t)$ crosses over the free diffusion to meet the $g_{cm}(t)$ of the same N and then $g_i(t) = g_{cm}(t)$. The shorter the chain length, the earlier $g_i(t)$ crosses over. However, it is notably apparent that there is a clear plateau for the values of $g_i(t)$ divided by $t^{8/15}$, as shown in Fig. 6(b) in comparison to the slight slope of $g_i(t)$ divided by $t^{1/2}$ as shown in Fig. 6(a). This result indicates that the correlation between the relaxation time and the chain length is likely $t_N \sim N^{15/8}$. The chain diffusion dynamics of the polymer melts in strictly two dimensions of our model obey a near-Rouse power law. Our simulation results can completely approve the prediction of Semenov and Johner.¹

It should be noted that there are some arguments on whether or not the DPD model can describe the correct dy-

namical behavior of real polymers. Groot and Warren⁴ first discussed the application of DPD to simulate the dynamics of the mesoscopic systems. Specifically, they focused on the Schmidt number $Sc = \nu/D$ in which ν is the kinematic viscosity and D is the diffusion constant. For a normal fluid, the momentum diffusion is always faster than the particle mass diffusion as a consequence of the caging effect of the interparticle potential. Thus, the hydrodynamic interactions can be established in the time scale of the particle motion, which is essential to the Zimm²⁸ model of polymer dynamics. However, in DPD, Sc is highly reduced because of the usage of the ultrasoft potentials, which are about three orders of magnitude lower than that of a real fluid. Such a small value implies that particles are diffusing as fast as the momentum in the DPD fluid. As a result, whether the DPD method can correctly describe the Zimm dynamics is unclear. However, Peters²⁹ indicated that Sc may be an ill-defined quantity in a coarse-grained approach. At this point, Jiang *et al.*¹⁰ indicated that the use of soft interaction between the polymer beads and a low Sc had not produced noticeable problems for the simulated dilute polymer solution dynamics. Under the typical DPD simulation conditions, they found that in dilute polymer solution, the Zimm scaling is obeyed very well.

Apparently, the DPD method should correctly describe the Rouse dynamics. In the past decade, this was well verified by a series of papers. For example, in Ref. 8, Spensley simulated the polymer melts by DPD, and the results could be fitted well by Rouse scaling. The usage of the ultrasoft potential in the DPD also shows that the particles are possibly penetrable and the bond crossings take place. Consequently, the reptation dynamics cannot be described in the conventional DPD. The work of Nikunen *et al.*¹⁹ was a minimal modification of DPD, which avoids the bond crossing so that for longer chains the dynamics becomes reptational in melt.

Although all three important polymer dynamic scalings can be described in the framework of DPD, the specific dynamics of a real polymer, however, cannot be described well with DPD since the DPD interaction is aimed to map on Flory–Huggins theory. Inherently, it corresponds to a high-level coarse graining without any consideration of the dynamics of a specific polymer chain. Compared with real polymers, the momentum diffusion is reduced, and the particle mass diffusion is enhanced at this coarse-graining level due to the usage of ultrasoft potentials. Therefore, if we want to study the real dynamics of a specific polymer, systematic bottom-up coarse graining is needed. The most successful examples include Kremer's works (see the recent review³⁰ and references therein). As a consequence, the coarse-graining level is (partially) decreased. If we want to retain the coarse-graining level of DPD, we can only minimally modify the DPD soft potential with which some of the inherent problems in the conventional DPD such as bond crossing can be solved, but not totally. To investigate the real polymer dynamics, a correct bottom-up coarse graining is a must. But the conservative interactions are not linear anymore, and their mapping onto the Flory–Huggins theory may fail. That is actually the dilemma in the field of mesoscale simulations.

Therefore, the multiscale simulation techniques, which can correctly describe the polymer thermodynamics and dynamics as well, are highly favored.

IV. CONCLUSIONS

Because of the soft interactions between particles in dissipative particle dynamics, it inevitably cause bond crossing among the different bonds and overlaps between different particles. Here, we have developed a practical method based on the DPD model that can reasonably avoid bond crossing. In this method, we add a rigid core to each particle by modifying the form of the conservative force in DPD so that the particles cannot overlap with each other. A preset maximum force with value F_{\max} is added to the conservative force when the distance between two particles are small enough to ensure that every DPD particle has a rigid core that is impenetrable. When the distance between a pair of particles r_{ij} is less than the preset rigid core diameter $2r_0$, both of the two particles will suffer the maximum force F_{\max} . The RDF is then used to check the actual value of the rigid core radius, which is further used for fine-tuning the rigid core size. We refer to the simple geometry constraint conditions in three and two dimensions, respectively, to design the condition of avoiding bond crossing in polymer chains. We find that if the rigid core radius r_0 and the maximum value of the bond length of the polymers l_{\max} can satisfy the relationship $\sqrt{2} \cdot 2r_0 > l_{\max}$ in three dimensions and $4r_0 > l_{\max}$ in two dimensions, the bond crossing can be absolutely avoided. We have to increase the spring constant C to a proper value to make sure that the maximum bond length l_{\max} is short enough to satisfy the relations above.

We further use an analytic geometry method together with the idea of polymerization to solve a key problem in two dimensions that avoids the bond crossing during the process of polymer bond generation. Here, we consider the bonds as line segments in the analytical geometry to find the condition that the pair of line segments has a meeting point. Then we can avoid the possibility of the newly generated bond crossing with the preexisting bonds just by prohibiting the line-segment-meeting condition in our algorithm. The whole algorithm is proved to be feasible, and we have obtained the chain configurations that are good starting points for further simulations in two dimensions.

We have also checked some characteristic parameters to validate our modified DPD model. By a parabola fitting between the pressure and the particle number density, we find that our model with small r_s can still be mapped onto the

Flory–Huggins-type model, and the mesoscopic length scale of our simulations does not change. By analyzing the MSDs of the center of mass $g_{\text{cm}}(t)$ and the innermost monomer of the chains $g_i(t)$, we find a near-Rouse power law in our model, i.e., $g_i(t) \sim t^{8/15}$, which agrees well with the prediction of Semenov and Johner¹ but is in contrast to the prediction of $t^{1/2}$ in the Rouse theory.

ACKNOWLEDGMENTS

This work was supported by NSFC (Grant Nos. 20490220 and 20774036) and Fok Ying Tung Education Foundation (Grant No. 114018).

- ¹A. N. Semenov and A. Johner, *Eur. Phys. J. E* **12**, 469 (2003).
- ²Y. Shapir and Y. Oono, *J. Phys. A* **17**, L39 (1984).
- ³H. Meirovitch, I. S. Chang, and Y. Shapir, *Phys. Rev. A* **40**, 2879 (1989).
- ⁴R. D. Groot and P. B. Warren, *J. Chem. Phys.* **107**, 4423 (1997).
- ⁵R. D. Groot and T. J. Madden, *J. Chem. Phys.* **108**, 8713 (1998).
- ⁶P. V. Coveney and K. E. Novik, *Phys. Rev. E* **54**, 5134 (1996).
- ⁷K. E. Novik and P. V. Coveney, *Phys. Rev. E* **61**, 435 (2000).
- ⁸N. A. Spenley, *Europhys. Lett.* **49**, 534 (2000).
- ⁹M. Lísal, J. K. Brennan, and W. R. Smith, *J. Chem. Phys.* **125**, 164905 (2006).
- ¹⁰W. H. Jiang, J. H. Huang, Y. M. Wang, and M. Laradji, *J. Chem. Phys.* **126**, 044901 (2007).
- ¹¹P. Malfreyt and D. J. Tildesley, *Langmuir* **16**, 4732 (2000).
- ¹²C. M. Wijmans and B. Smit, *Macromolecules* **35**, 7138 (2002).
- ¹³H. J. Qian, Z. Y. Lu, L. J. Chen, Z. S. Li, and C. C. Sun, *Macromolecules* **38**, 1395 (2005).
- ¹⁴H. J. Qian, L. J. Chen, Z. Y. Lu, and Z. S. Li, *Phys. Rev. Lett.* **99**, 068301 (2007).
- ¹⁵W. Liu, H. J. Qian, Z. Y. Lu, Z. S. Li, and C. C. Sun, *Phys. Rev. E* **74**, 021802 (2006).
- ¹⁶J. T. Padding and W. J. Briels, *J. Chem. Phys.* **115**, 2846 (2001).
- ¹⁷P. Kindt and W. J. Briels, *J. Chem. Phys.* **123**, 224903 (2005).
- ¹⁸G. Pan and C. W. Manke, *Int. J. Mod. Phys. B* **17**, 231 (2003).
- ¹⁹P. Nikunen, I. Vattulainen, and M. Karttunen, *Phys. Rev. E* **75**, 036713 (2007).
- ²⁰P. Español and P. B. Warren, *Europhys. Lett.* **30**, 191 (1995).
- ²¹V. Ortiz, S. O. Nielsen, D. E. Discher, M. L. Klein, R. Lipowsky, and J. Shillcock, *J. Phys. Chem. B* **109**, 17708 (2005).
- ²²H. Liu, H. J. Qian, Y. Zhao, and Z. Y. Lu, *J. Chem. Phys.* **127**, 144903 (2007).
- ²³H. Meyer, T. Kreer, A. Cavallo, J. P. Wittmer, and J. Baschnagel, *Eur. Phys. J. Spec. Top.* **141**, 167 (2007).
- ²⁴A. Cavallo, M. Müller, and K. Binder, *Europhys. Lett.* **61**, 214 (2003).
- ²⁵M. P. Allen and D. J. Tildesley, *Computer Simulation of Liquids* (Clarendon, Oxford, 1987).
- ²⁶L. E. Reichl, *A Modern Course in Statistical Physics* (University of Texas, Austin, 1980).
- ²⁷M. Rubinstein and R. H. Colby, *Polymer Physics* (Oxford University Press, Oxford, 2003).
- ²⁸B. H. Zimm, *J. Chem. Phys.* **24**, 269 (1956).
- ²⁹E. A. J. F. Peters, *Europhys. Lett.* **66**, 311 (2004).
- ³⁰M. Praprotnik, L. D. Site, and K. Kremer, *Annu. Rev. Phys. Chem.* **59**, 545 (2008).